 MCB, vol.8, no.4, pp.275-296, 2011

Structure - Function Relationships in the Stem Cell's Mechanical World A: Seeding Protocols as a Means to Control Shape and Fate of Live Stem Cells

Joshua A. Zimmermann* **and Melissa L. Knothe Tate*,†,‡**

Abstract: Shape and fate are intrinsic manifestations of form and function at the cell scale. Here we hypothesize that seeding density and protocol affect the form and function of live embryonic murine mesenchymal stem cells (MSCs) and their nuclei. First, the imperative for study of live cells was demonstrated in studies showing changes in cell nucleus shape that were attributable to fixation *per se*. Hence, we compared live cell and nuclear volume and shape between groups of a model MSC line (C3H10T1/2) seeded at, or proliferated from 5,000 cells/cm^2 to one of three target densities to achieve targeted development contexts. Cell volume was shown to be dependent on initial seeding density whereas nucleus shape was shown to depend on developmental context but not seeding density. Both smaller cell volumes and flatter nuclei were found to correlate with increased expression of markers for mesenchymal condensation as well as chondrogenic and osteogenic differentiation but a decreased expression of pre-condensation and adipogenic markers. Considering the data presented here, both seeding density and protocol significantly alter the morphology of mesenchymal stem cells even at very early stages of cell culture. Thus, these design parameters may play a critical role in the success of tissue engineering strategies seeking to recreate condensation events. However, a better understanding of how these changes in cell volume and nucleus shape relate to the differentiation of MSCs is important for prescribing precise seeding conditions necessary for the development of the desired tissue type. In a companion study (Part B, following), we address the effect of concomitant volume and shape changing stresses on spatiotemporal distribution of the cytoskeletal proteins actin and tubulin. Taken together, these studies bring us one step closer to our ultimate goal of elucidating the dynamics of nucleus and cell shape change as tissue

* Department of Biomedical Engineering, Case Western Reserve University, 2071 Martin Luther King Drive, Cleveland, OH 44106-7207

† Department of Mechanical & Aerospace Engineering, Case Western Reserve University, 2123 Martin Luther King Drive, Cleveland, OH 44106-7207

‡ Corresponding author. Phone: (216)-368-5884; Fax: (216)-368-4969; knothetate@case.edu

templates grow (cell proliferation) and specialize (cell differentiation).

Keywords: developmental biology, mechanobiology, tissue engineering, regenerative medicine, stem cell, density, proliferation, cell shape and volume, nucleus shape and volume, fate, differentiation, mechanical cues

1 Introduction

The targeted differentiation of pluripotent stem cells and the subsequent secretion of extracellular matrix proteins appropriate for the desired tissue is an important step in the development of organisms *in utero* in addition to the *de novo* engineering of tissue. In recent years, the concept of epigenetics, the study of changes in cell phenotype due to mechanisms other than a change in DNA, has become increasingly important in determining how complex organisms arise from a single genome. During development, both biochemical and mechanical signals play a role in guiding cell fate. Although biochemical cues modulating stem cell fate have been identified, the biophysical (mechanical) cues conducive to guiding stem cell fate are less well understood.

During mesenchymal condensation, the initial step of skeletogenesis which occurs prior to the first beat of the heart or twitch of skeletal muscle, transduction of minute ($1000\times$ smaller than forces incurred through weight bearing) mechanical forces to the nucleus is associated with up or down-regulation of genes, ultimately resulting in formation of the skeletal template and appropriate cell lineage commitment [15]. The summation of these biophysical cues experienced by the cell largely affects the cell's morphology and shape. In fact, numerous biophysical cues have been show to influence cell and nucleus shape including cell density [19,20], deviatoric shear stress [21], osmotic stress [10], and the mechanical compliance of the cell's environment [6]. However, this cell scale structure (form, shape) and function (fate) relationship has not yet been well characterized.

Our previous studies demonstrate that cell and nucleus shape influence the commitment of mesenchymal stem cells to a particular fate [20]. Together with other recent studies [7,14], these studies provide a proof of principle to modulate stem cell shape and fate through control of the target density at which cells are seeded and the manner in which density is achieved [20]. For instance, a rounding of the nucleus of fixed MSCs is observed in cells seeded at 5,000 cells/cm^2 and proliferated to very high density (86,500 cells/cm^2) but not in cells seeded directly at that target density or cells seeded at or proliferated from 5,000 cells/cm^2 to lower densities. Furthermore, significant changes in baseline expression of *Sox9* and Aggrecan, genes marking mesenchymal condensation and the start of chondrogenesis, are observed only in experimental groups showing significant rounding of the nu-

cleus and not in other seeding groups [20].

Given the results of our previous study in *fixed* cells, the elucidation of seeding protocols to achieve targeted developmental contexts for multipotent cells may provide a new avenue to effect targeted cell differentiation and tissue self assembly [20]. However, in order to study adaptation of cells over time, it is important to study structure-function relationships in living cells. To the best of our knowledge, no studies to date have examined cell and nuclear shape and its role in mechanical adaptation of the stem cell to its local mechanical environment in *living* MSCs, providing the impetus for the current study. We hypothesize that biophysical cues, induced through seeding density and protocol, modulate the shape of live murine mesenchymal stem cells and their nuclei. Furthermore, we hypothesize that these cell and nuclear shape changes correlate to changes in expression of genes marking mesenchymal condensation and the commitment of mesenchymal stem cell fate. Our approach was to measure the effect of seeding density and protocol on cell and nuclear shape using live cell imaging methods.

2 Materials and Methods

2.1 Overview

Ideally, we would use primary embryonic mesenchymal stem cells derived from the mesodermal core at pericondensation time points to assess the role of cell density and seeding protocol on the adaptation of stem cells to biophysical cues in the context of mesenchymal condensation. However, primary cells are difficult to obtain in sufficient quantities and they exhibit phenotypic drift when cultured [8,16]. Thus, we opted to use the C3H/10T1/2 cell line of murine multipotent embryonic cells derived from the mesenchyme (CCL-226; ATCC, Manassas, VA), a cell line with which our lab has significant prior experience and reference data [20,21,23]. The C3H/10T1/2 model mesenchymal stem cell line has been shown to be capable of differentiating along several lineage paths, including osteogenic, chondrogenic, adipogenic, smooth muscle [13,22,24] and endothelial cell fates [25].

To achieve targeted developmental contexts for multipotent cells, analogous to our previous studies [20], we used the three target seeding densities, which were based on the growth curve of this cell line as well as previous studies designed to create tissue templates with properties specific to pre-, peri-, and post-mesenchymal condensation events. In addition to seeding density, we used two means of achieving target density, which controlled the initial boundary conditions and hence mechanical environment of the cell [20]. Cells at low density (LD, 16,500 cells/cm^2,Figure 1A) were expected to be very isolated, with little contact to neighboring cells. In contrast, cells at very high density (VHD, 86,500 cells/cm^2, Figure 1A) were ex-

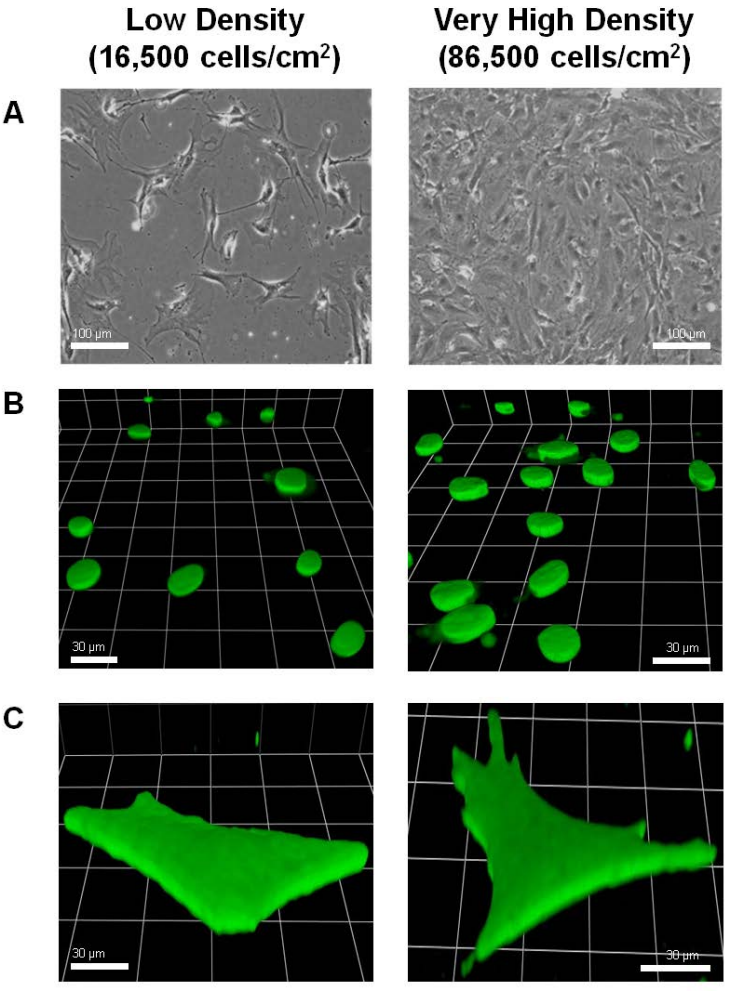

Figure 1: **Seeding density and protocol impacts nucleus shape and cell volume.** (A) Phase contrast image at 40x magnification. Low density seeding results in very few cell-cell contacts while very high density seeding results in a confluent cell layer. Three dimensional renderings of SYTO 9 labeled nuclei (B) and Organelle Lights – Cyto GFP™ transfected cells (C) created by reconstruction in three dimensions image stacks acquired using confocal microscopy. Note: Due to the low transduction efficiency of the Organelle Lights reagent, fluorescent images do not show all the seeded cells, only those successfully tagged with the fluorescent protein.

pected to be near confluent, as this density occurs just prior to the plateau phase of the growth curve of the C3H/10T1/2 cells [19]. Cells at high density (HD, 35,000 cells/cm^2) were expected to experience an environment between these two extremes, where cells may be in contact with one another yet still have room to proliferate and spread. In addition to these seeding densities, two seeding protocols were used to alter the developmental context in which the cells reach the target densities. Cells were either seeded directly at the three target densities or seeded at a very low density (5,000 cells/cm^2) and allowed to proliferate to the target densities. Thus, cells seeded using these protocols differed in the time cells had to adapt to their environment as well as in that their initial boundary conditions were prescribed by surrounding cells or lack thereof when seeded at density or by neighboring cells and increasing space constraints as they proliferated to the target densities.

2.2 Cell Culture and Seeding Protocols

C3H/10T1/2 multipotent progenitor cells were passaged in growth medium (Basal Medium Eagle supplemented with 10% fetal bovine serum, 1% L-Glutamine, and 1% Penicillin/Streptomycin [Invitrogen, Carlsbad CA]) and incubated at 37^{o}C and 5% CO_2 in a humidified incubator until passage 3 (P3). At P3, cells were stored in medium with 40% fetal bovine serum and 10% DMSO at -80^{o}C until needed. Before use, one more passage was allowed, bringing cells in all experiments to P5. Cells were seeded on 2.5 cm diameter glass coverslips (Fischer Scientific, Hampton, NJ) that were sterilized prior to use. Glass coverslips were chosen as a biologically and chemically neutral surface that has the practical advantages of being readily integratable into our custom design *in situ* live imaging chamber that allows for precise control of the cellular environment, including biochemical and biophysical gradients [1,2].

One group of C3H/10T1/2 cells were seeded at the three target densities and given 24 hours to adhere to the coverslip. The second group of C3H/10T1/2 were seeded at 5,000 cells/cm^2 and given 3, 4, and 5 days to proliferate in order to reach the LD, HD, and VHD groups, respectively. Additionally, in order to get a clearer picture of how mesenchymal stem cells adapt to these prescribed seeding conditions, a third seeding method was used to evaluate cell shape and volume, where cells were seeded at half the target densities so that they reached the desired density after two days in culture. This provides a developmental context on a time scale between the experimental groups where cells were seeded at target density or proliferated to density. Finally, cells seeded at the three target densities were evaluated after several days in culture to determine if cell and nucleus shape and volume were persistent over time as cells seeded at these densities proliferated to confluency.

Cells were seeded at LD, HD, and VHD and were evaluated after 5, 4, and 3 days in culture respectively, the time it takes cells seeded at these densities to reach a confluent state where cell density is no longer changing. Cell density was measured using a hemocytometer.

2.3 Cell Staining

To measure the shape of cells and their nuclei as they adapt to the seeding conditions, the nucleus and cytoplasm of cells were fluorescently labeled using agents specific to these areas of the cell. To evaluate nucleus shape, the nuclear stain SYTO 9 (Invitrogen, Figure 1B) was applied to cells Alternatively, to evaluate cell shape, the cytoplasm of cells were labeled using Organelle Lights-Cyto GFP™ (Invitrogen, Figure 1C), a reagent that uses the BacMam delivery technology to direct the expression of autofluorescent proteins specific to the cytoplasm of the cell. The Organelle Lights reagent was applied to the cells according to the manufacturer's protocol. It was found that this procedure affects neither the attachment of cells to the coverslip nor achievement of the target densities. The transfection rate was 30-50%, depending on cell density, which enabled us to visualize individual cells without the inherent challenge of distinguishing between touching or overlapping cells. Both the nuclear stain SYTO 9 and the Organelle Lights reagent stain the cell nucleus and cytoplasm, respectively, without the need for permeabilization of the cell; as a result, cells remain alive throughout the staining process and can be imaged without prior fixation.

2.4 Three-Dimensional Live Cell Imaging and Analysis

A high resolution laser scanning confocal microscope (SP2, Leica Microsystrems, Mannheim Germany) was used for imaging in three dimensions. One randomly chosen field of view was imaged per coverslip at 40x magnification and every cell and nucleus found within this field of view was counted. For nucleus measurements, three coverslips were imaged for each seeding density and protocol combination. For cell measurements, we measured cells on five coverslips to insure adequate sample size (due to imperfect transfection rate of the Organelle Lights reagent). By rendering of the stacks of planar images, we reconstructed the shape of the nucleus and overall cell shape in live cells.

The images were post-processsed and analyzed using Volocity (Improvision, Coventry, England). Cell and nuclear volume as well as surface area were calculated for cells in order to evaluate the shape of the cell and nucleus for each of the seeding density and protocol groups. The ratio of surface area to volume (SA/V) has previously been used as a measurement of cell and nucleus shape [20]. However, this measurement of shape is dependent on the volume of the object, and thus two ob-

jects with the same shape but different volume will have two different SA/V ratios. In order to get measurements of shape independent of cell volume, the surface area to volume ratio of each cell was normalized to the surface area to volume ratio of a sphere with the same volume. This normalized SA/V gives a measurement of the shape of the cell compared to a sphere, with a value of 1 indicating a perfect sphere and a greater value indicating a flatter, more spread cell. In addition to the normalized surface area to volume ratio, cell height was used as an additional, independent outcome measure for the shape of the entire cell.

2.5 Statistical and Correlation Analysis

Statistical analysis was performed using Excel (Microsoft) and JMP (SAS Institute Inc, Cary NC) to determine significant differences in shape between seeding density and seeding protocol groups. The data was compared using a Wilcoxon rank sum test and defined as significant if the p-value was less than or equal to 0.05. In addition, a non-parametric, multivariate correlation analysis (Spearman's ρ, JMP, SAS Institute Inc, Cary NC) was performed between measurements of live cell and nucleus shape and volume and previously reported fixed cell and nucleus shape and volume as well as real time PCR data of C3H/10T1/2 cells seeded using the same protocols described here [20]. Previously, changes in gene expression due to varying seeding density and protocol was measured to determine if these conditions could alter expression of mesenchymal condensation markers as well as markers of osteogenic, chondrogenic, and adipogenic differentiation (Fig. 2). Specifically, *Msx2* and type I collagen (*ColIa1*) were assessed, as these genes are markers of the relative stage of (pre-, respectively, peri-) mesenchymal condensation [9,15]. Additionally, *Runx2* was measured as a marker of osteogenic differentiation (in absence of *Msx2*) and while *Sox9*, and type II collagen (*ColIIa1*) as well as Aggrecan (AGC) were measured as markers of early as well as later chondrogenic differentiation, respectively. Finally, peroxisome proliferation activated receptor-γ2 (*Pparγ2*) was measured as a marker of adipogenic differentiation [15]. Correlation coefficients were calculated between each of these seven genes and the measurements of cell and nucleus shape and volume and coefficients were defined as significant if its p-value was less than or equal to 0.05.

3 Results

3.1 C3H10T1/2 Growth Characteristics

To determine whether intrinsic difference in proliferation state among experimental groups could account for observed differences in cell volume or nucleus shape, we charted cell densities versus time in culture for experimental groups seeded

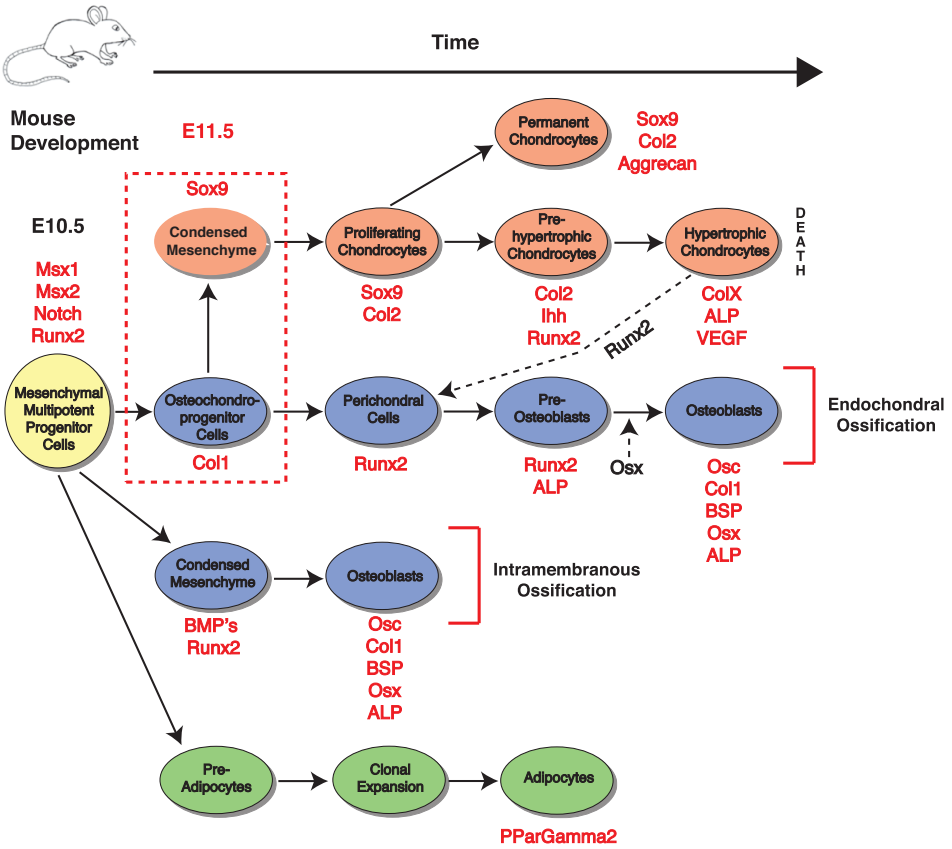

Figure 2: **Patterns of gene expression indicative of relative stage in lineage commitment over time.** Genetic markers (red text) indicative of relative state with reference to mesenchymal condensation (red dotted square, at approximately E11.5 in murine embryos), and chondrogenic (orange), osteogenic (blue), as well as adipogenic (green) paths toward lineage commitment. Used with permission from [15].

at 5,000, 16,500, 35,000, and 86,500 cells/cm^2 (Figure S0). All experimental cohorts reached the same steady state, comprising a density of approximately 120,000 cells/cm^2. Furthermore, for equivalent densities, the growth rate of the cells at each of the density and time in culture groups (as measured by the slope of the curve) was approximately parallel and thus similar. These data confirm that differences in cell or nuclear shape, within the range of densities examined, are not attributable to

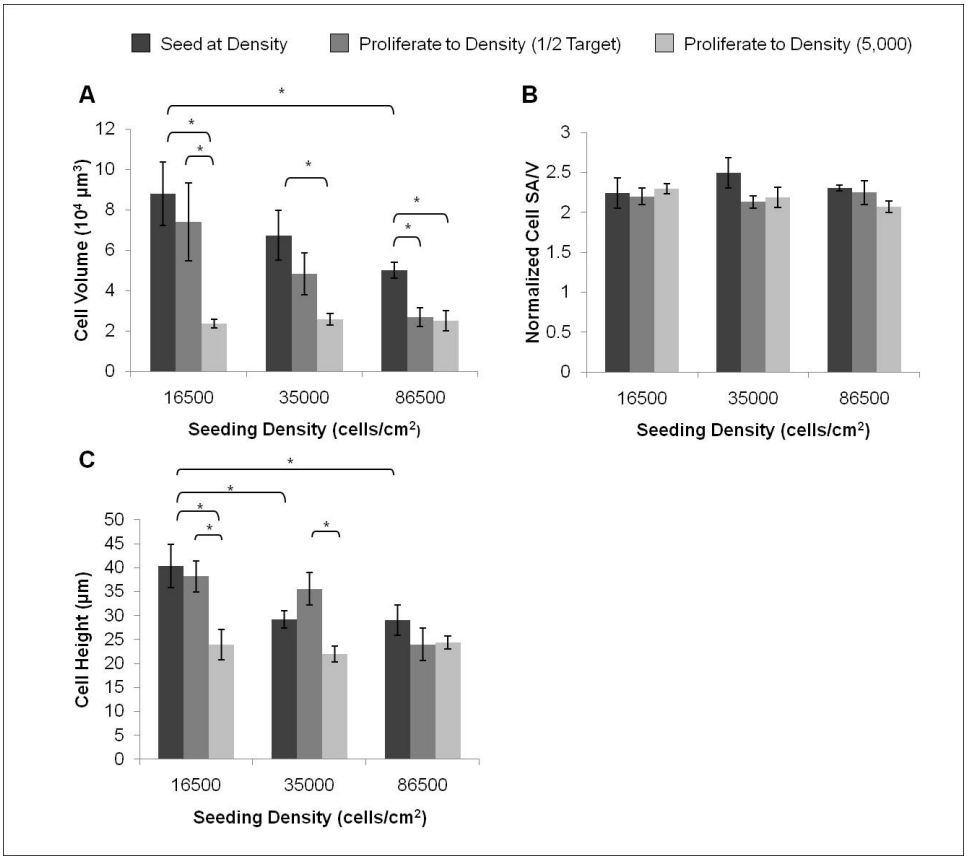

Figure 3: **Measures of cell volume and shape as a function of different seeding densities and mode of achieving target density.** (A) For the live cells, significant differences ($p < 0.05$) in cell volume are observed between cells seeded at low density and cells grown to the three target densities and cells seeded at very high density. (B) No significant differences in cell shape, measured as the normalized surface area to volume ratio of the cell, are observed between cell densities or seeding conditions. (C) Significant differences ($p<0.05$) are observed in cell height. Cells seeded at low and high densities were taller than cells grown to density or seeded at very high density. For all seeding density and protocol groups, n=5.

intrinsic differences in proliferation rate or stage between groups at similar densities albeit different means of achieving density (seeding protocol).

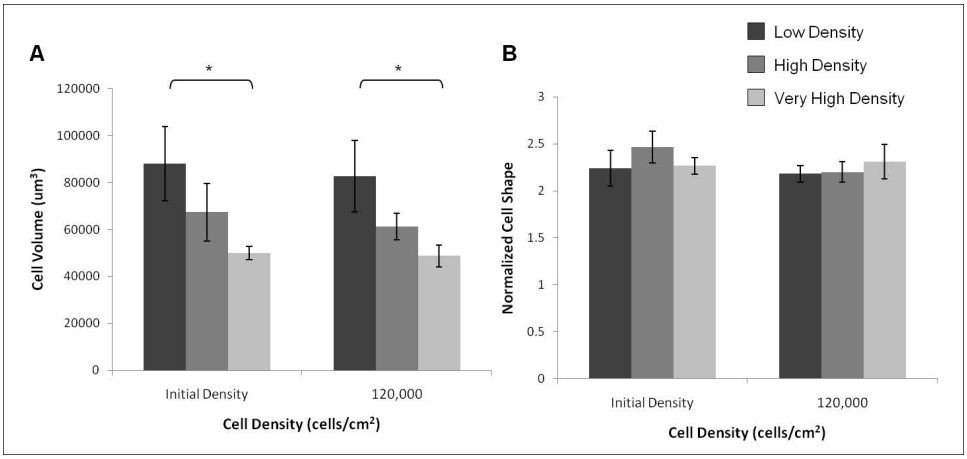

Figure 4: **Comparison of cell volume and shape at initial and final (confluent) time points, e.g. C3H10T1/2 cells seeded at LD, HD, and VHD (Initial Density) and after cells seeded at these densities have proliferated to the maximum confluent state (120,000).** (A) No significant differences ($p < 0.05$) in cell volume are observed between cells at their initial cell density and at 120,000 cells/cm^2 for each of the initial seeding densities. (B) No significant changes in cell shape were observed between cells at the initial cell density and after proliferating to 120,000 cells/cm^2.

3.2 Cell Shape and Volume

The density and developmental context of seeded stem cells exerts a significant effect on cell volume (Figure 3A) but not on cell shape (Figure 3B, as measured by the surface area to volume ratio, with a greater SA/V indicating a flatter cell). Cell volume was found to decrease as cell density increased and was also found to decrease with time spent in culture to achieve the target density (Figure 3A). However, cell volume did not differ between cells that were proliferated to achieve target density, indicating that over longer periods of time, initial cell density rather than actual cell density modulates cell volume. In addition, it was observed that cell shape, when normalized to cell volume, did not significantly change in response to cell density or seeding conditions (Figure 3B). Cell height, measured from the lowest to highest point of the cell, was also found to be dependent on cell density and seeding protocol (Figure 3C). Cells that were seeded at both low density and high density were taller than cells that were grown to the target densities or seeded at very high density; these data are internally consistent, as the same cohorts of cells were found to have significantly larger volumes yet retained the same shape (Figure

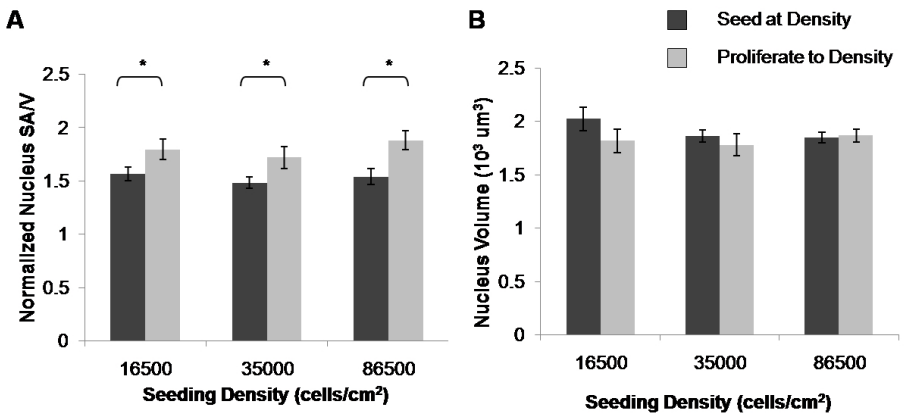

Figure 5: **Nucleus shape and volume for different seeding densities and mode of achieving target density.** (A) Shape is measured as the normalized surface area to volume ratio of the nucleus. For live cells, significant differences ($p<0.05$) are observed for each target density, between the two seeding protocols. (B) No significant differences in volume are observed between any of the seeding density and protocol groups. For the seeding at density protocol, n=24,65, and 127 for LD, HD, and VHD seeding densities respectively. For the proliferate to density protocol, n=27, 59, 122 for LD, HD, and VHD seeding densities respectively.

3C). No significant differences in height were found between cells seeded at low and high density. Finally, cell volume and shape was found to be persistent as cells seeded at the low, high, and very high densities proliferated to a maximum confluent state where no further cell proliferation occurs (Figure 4), with cells seeded at higher densities having significantly smaller volumes than those seeded at lower densities even at later time points. In sum, at higher densities, mesenchymal stem cells exhibit lower volumes, and over time, cells maintain a steady state volume, which depends on the initial density at which cells are seeded.

3.3 Nucleus Shape and Volume in Live Cells

Imaging of live cell nuclei subjected to different seeding densities and protocol shows that the shape of the nucleus, as measured by the surface area to volume ratio, depends on developmental context but not cell density (Figure 5A). Cells that proliferated to target density were found to have significantly flatter nuclei than cells that were seeded at the same target density. However, there were no

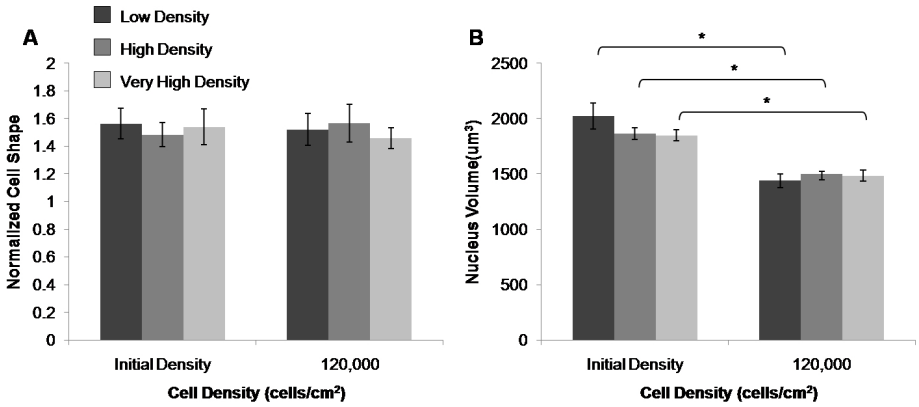

Figure 6: **Comparison of nucleus volume and shape at initial and final (confluent) time points, e.g. C3H10T1/2 cells seeded at LD, HD, and VHD (Initial Density) and after cells seeded at these densities have proliferated to the maximum confluent state (120,000).** (A) No significant changes in nucleus shape are observed between cells at the initial cell density and after proliferating to 120,000 cells/cm^2. (B). Nucleus volume decreases as cells reached 120,000 cells/cm^2 for each of the initial seeding densities.

significant differences in the shape of the nuclei of cells at low, high, or very high density if they were seeded using the same protocol (Figure 5A). Additionally, no significant differences were found in the volume of the nuclei of cells between any of the seeding density or seeding protocol groups (Figure 5B). Interestingly, while nucleus shape is persistent as cells seeded at low, high, and very high density proliferate to the maximum density state (Figure 6A), nucleus volume was found to be significantly smaller for all initial seeding densities (Figure 6B). Confluent (high density) cells are in a quiescent state as opposed to a proliferative state when initially seeded, which may account for changes in nuclear volume, as cells are no longer actively dividing.

3.4 Nucleus Shape and Volume in Fixed Cells

We also investigated the role of fixation on nuclear shape as measured by surface area to volume ratio (Fig. 7). Past studies have often used fixed MSCs when evaluating cell shape in response to biophysical cues. Crosslinking fixation agents, such as formaldehyde, are often used to crosslink proteins within the cell to preserve the cell's natural structure. However, fixation of cells in 3.7% formaldehyde prior

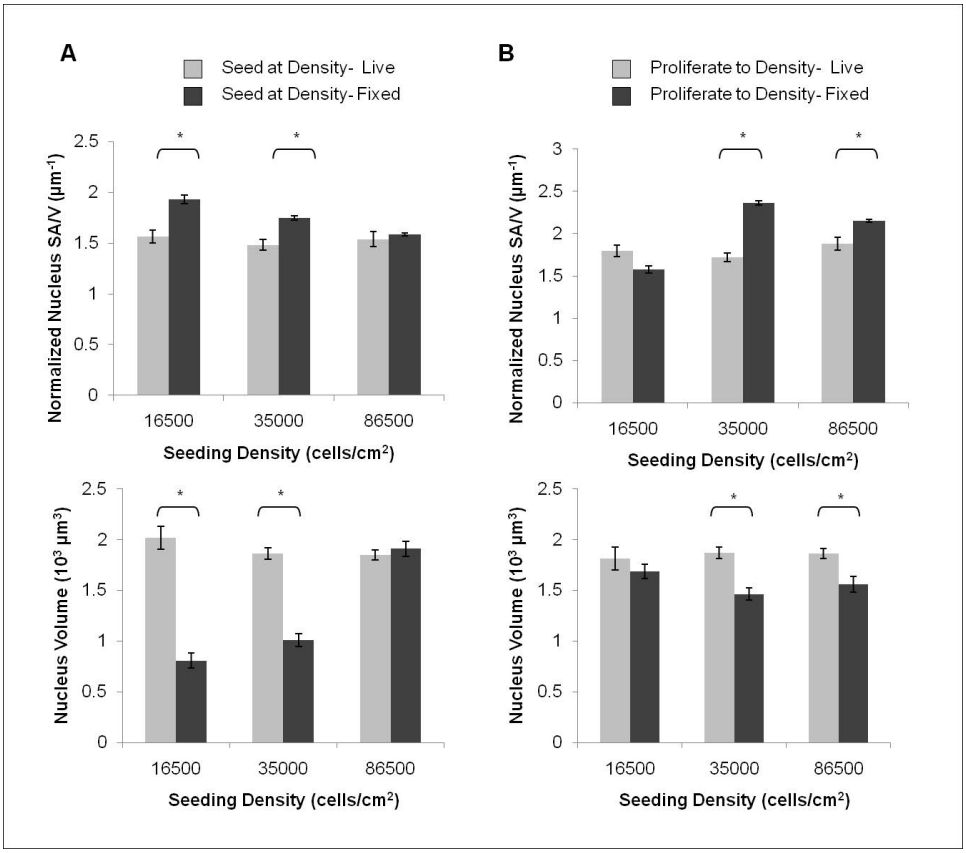

Figure 7: **Effect of cell fixation versus imaging of live cells.** Comparison of nucleus shape and volume for cells seeded at (A) and proliferated to (B) target densities. (A) Significant differences are observed in nucleus shape and volume between live and fixed cells seeded at all but the highest density (86,500 cells/cm^2). (B) Significant differences are observed in nucleus shape and volume between live and fixed cells at all but the cells proliferated to lowest density (16,500 cells/cm^2). In groups showing significant differences, fixation results in a decrease in nucleus volume (shrinkage) and a flattening in nucleus shape.

to imaging significantly altered the shape of their nuclei. The nuclei of fixed cells tended to increase in SA/V (flattening) and showed a decrease in volume compared to live cells. However, no significant difference in nuclear shape was found in cells grown to low density and seeded at very high density. Thus, fixation does appear to play a significant role in altering the shape and volume of the cell nucleus. More importantly, this artifact results in a change in nucleus shape that appears to be

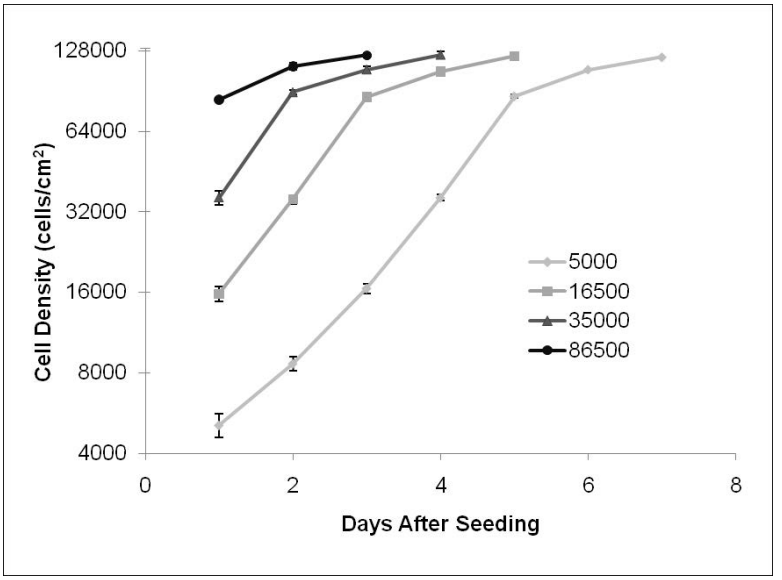

Figure S0: **Cell densities over time of C3H/10T1/2 cells seeded at 5,000, 16,500, 35,000, and 86,500 cells/cm^2 on a log$_2$ scale.** During the logarithmic growth phase, cells double approximately every day. Cells eventually reach an absolute confluency at approximately 120,000 cells/cm^2 regardless of initial seeding density. For experimental groups (i.e. seeded at or proliferated to LD, HD, and VHD), the proliferation rates are approximately parallel and thus similar.

directionally (apical - basal versus lateral) and environmentally (i.e. seeding density and developmental context) dependent. From the perspective of a cell, fixation causes the nucleus to decrease in volume, however, this change is not proportionally the same in all directions. The data shows that the nuclei flatten, indicating that the nucleus is losing more volume in the apical-basal direction compared to volume changes in the plane of the substrate. This fixation effect provides a previously unrecognized imperative to use live imaging protocols for MSC adaptation studies.

3.5 Correlation with Gene Expression

Previously reported real-time PCR data of C3H/10T1/2 cells seeded with the same protocols at the same target densities[20,21] was used in a correlation analysis to determine if changes in observed changes in live mesenchymal stem cell volume and nucleus shape correlate with changes in cell function and differentiation. Correlation coefficients and p-values for the correlation between each of the shape and

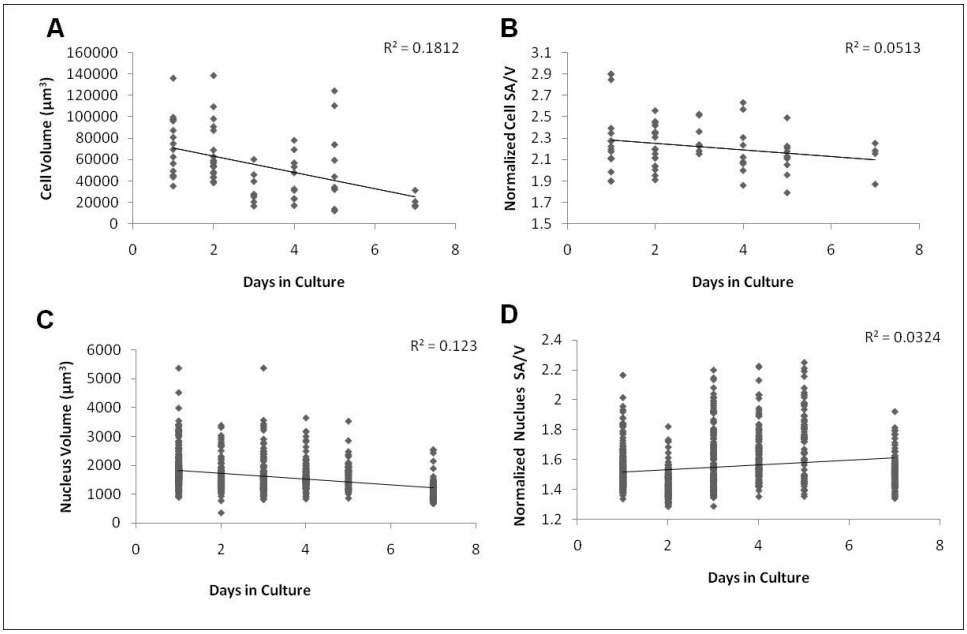

Figure S1: **Data pooled based on time spent in culture regardless of initial seeding density or actual cell density.** No significant trends ($R^2 > 0.80$) were observed in cell volume (A), cell shape (B), nucleus volume (C), or nucleus shape (D) when data was pooled in this manner.

volume measurements and the expression of each of these genes are displayed in Table 1. A larger cell volume was found to significantly correlate with a decreased expression of *ColI*, *Sox9*, *Runx2*, and *AGC* and an increased expression of *Pparγ* and *Msx2*. A flatter cell shape (larger SA/V) was found to correlate with a decreased expression of *ColI*, *Sox9*, *Runx2*, and *AGC*. In addition, a flatter nucleus shape significantly correlated with increased expression of *ColI*, *Sox9*, *Runx2*, and *AGC* and a decreased expression of *Pparγ* and *Msx2*. Finally, no significant correlations were found between nucleus volume and any of the measured genes.

3.6 Validation of Live Cell Measurement Techniques

To validate the methods of measuring cell and nucleus shape, the volume and surface area to volume ratio was calculated for nuclei using both xy planar images and orthogonal xz planar images. Due to differences in the microscope resolution between the xy and xz planes, similar measurements of nucleus shape obtained from these two sets of images would validate that no shape artifacts are being introduced

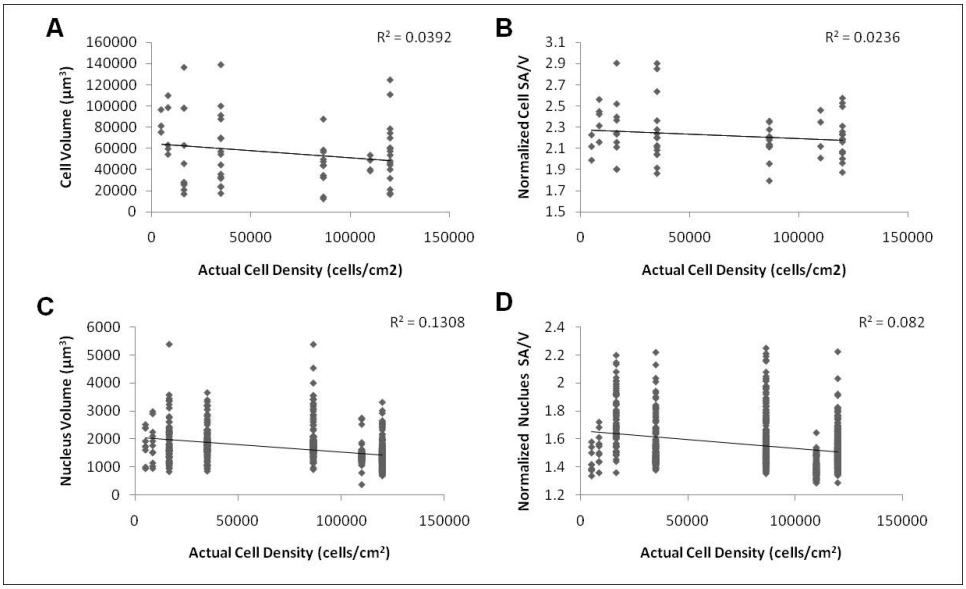

Figure S2: **Data pooled based on actual cell density at the time of morphology measurements regardless of initial seeding density or time spent in culture.** No significant trends ($R^2 > 0.80$) were observed in cell volume (A), cell shape (B), nucleus volume (C), or nucleus shape (D) when data was pooled in this manner.

by differences in resolution between orthogonal planes. In fact, it was found that the average percent difference in volume and SA/V between nuclei imaged using the two different methods was 3.0% $\pm$ 1.3% and 3.56% $\pm$ 1.2% respectively, indicating that these methods are accurate in measuring shape and volume.

4 Discussion

Based on the shape and volume data from the current study, biophysical cues, induced through cell seeding density and protocol, modulate the volume of mesenchymal stem cells as well as the shape of their nuclei. Furthermore, based on cross correlation analysis with gene expression data from a previous study using identical cell seeding protocols, these changes in cell volume and nucleus shape correlate significantly with changes in expression of genes marking mesenchymal condensation and the commitment of mesenchymal stem cell fate, including osteogenic, chondrogenic and adipogenic differentiation. Specifically, seeding mesenchymal stem cells at increasing target density is associated with a concomitant decrease in cell volume, reaching a steady state, with time, that depends on the

Table 1: Correlation analysis to elucidate relationships between cell and nucleus morphology and expression of genetic markers indicating mesenchymal condensation state (pre-condensation: Msx2, peri-condensation: *Col1A, Sox9*, post-condensation: *Col2A*) as well as chondrogenic (*Sox9, AGC Aggrecan*), osteogenic (*Runx2*), and adipogenic differentiation (*Pparγ*). Spearman's ρ correlation coefficients and p-values between measurements of live cell and nucleus shape and volume and previously reported real time PCR data. Statistically significant correlations (p-value < 0.05) are highlighted in green and lack of significance is indicated by pink highlighting.

Correlation Analysis												
Correlation Coefficients		Morphology Measurements				Relative Fold Change in Expression of						
		CV	CS	NV	NS	Col1A	Sox9	Col2A	Runx2	Aggrecan	PparG	Msx2
Morphology Measurements	Cell Volume	X	0.3517	0.0147	-0.498	-0.4642	-0.3081	0.0505	-0.3725	-0.2532	0.1926	0.3272
	Cell Shape	0.3517	X	-0.0165	-0.4308	-0.3273	-0.3193	0.1548	-0.3739	-0.2546	0.0654	0.0324
	Nucleus Volume	0.0147	-0.0165	X	-0.0519	-0.0859	-0.036	-0.0003	-0.0353	-0.1172	0.0685	0.0651
	Nucleus Shape	-0.498	-0.4308	-0.0519	X	0.4639	0.5712	0.0499	0.5456	0.3945	-0.229	-0.2264
P-values		Morphology Measurements				Relative Fold Change in Expression						
		CV	CS	NV	NS	Col1A	Sox9	Col2A	Runx2	Aggrecan	PparG	Msx2
Morphology Measurements	Cell Volume	X	<.0001	0.8734	<.0001	<.0001	0.0006	0.5841	<.0001	0.0053	0.0351	0.0003
	Cell Shape	<.0001	X	0.8579	<.0001	0.0003	0.0004	0.0913	<.0001	0.005	0.4777	0.7251
	Nucleus Volume	0.8734	0.8579	X	0.5733	0.3512	0.6961	0.9978	0.702	0.2025	0.4569	0.4798
	Nucleus Shape	<.0001	<.0001	0.5733	X	<.0001	<.0001	0.5887	<.0001	<.0001	0.0119	0.0129

initial seeding density. In contrast, the shape of the cell nucleus but not its volume, depends significantly on developmental context but not on seeding density, where cells seeded at identical densities and then proliferated to target density exhibited flatter nuclei than cells seeded directly at target density. Furthermore, these cell volume and nucleus shape changes correlate significantly with very early markers [15,20,21] of stem cell fate decisions. Namely, larger cell volumes (observed when seeding at lower initial target densities) as well as flatter nuclei (observed in cells proliferated to target densities) correlate with increased expression of markers for mesenchymal condensation *(ColI, Sox9)*, chondrogenesis *(Sox9,AGC)* and osteogenesis *(Runx2)*, but a decreased expression of markers for the pre-condensation state (*Msx2*) and adipogenesis (*Pparγ*). Finally, changes in nucleus shape attributable to cell fixation provide a previously unrecognized imperative to use live imaging protocols for MSC adaptation studies.

Interestingly, from a mechanics perspective, considering that cell surface integrin receptors, cytoskeletal filaments, and nuclear scaffolds are mechanically coupled in living cells [4,18], the cell and its nucleus respond differently to the same global mechanical environment. On the one hand, the difference in response may reflect real differences in the local (subcellular) mechanical environment (force balance) at the surface of the cell and the nucleus [23]. On the other hand, differences may

reflect inherent anisotropies in material properties at the subcellular scale. While cells proliferating to higher densities appear to experience dilatational (volume changing) stresses, the nucleus appears to experience deviatoric (shape changing) stresses. This may be due to the greater stiffness of the nucleus compared to the cell cytoplasm [12] as well as the inherent anisotropy of the cytoskeleton linking the outer boundary of the cell to the nuclear envelope. Both the cell and the nucleus appear to reach an equilibrium state over the same time period, suggesting a connection between these two adaptations. As these cells spend more time in culture, the cell decreases in volume and the nucleus flattens. The decrease in cell volume may be influencing this change in nuclear shape, potentially due to a decrease in cytoplasm buffering around the nucleus resulting in it sensing a stiffer matrix or due to an increase in cytoskeletal element concentration around the periphery of the nucleus resulting in a change in the distribution of intrinsic cytoskeletal forces (a hypothesis which we test in the follow on study, Part B). Interestingly, these results may suggest that while the cell may adapt itself or its extracellular environment to reduce stress experienced at its boundary, the cell may also adapt itself to reduce the stress experienced by the nucleus at its boundary with the rest of the cell, our current working hypothesis which were test by visualizing and measuring stress experienced in live cells over time using microbead displacement [23]. Hence, while cell volume may play a role in influencing nucleus shape, multiple other mechanisms may be involved in influencing nuclear shape under these conditions.

Living cells experience shape and volume changes independent of deviatoric and dilatational stresses, *e.g.* due to biochemical changes in the culture media (which was controlled for in the current study) or due to paracrine signaling effects, *e.g.* as cell-cell contacts increase at higher densities (which could not be controlled for in the current study). In addition, changes in substrate compliance [6] (controlled for in this study by using a biochemically neutral, stiff glass coverslip), as well as cell-cell junctions, cell-substrate junctions, and other factors not controlled for in the current study may influence cell shape and fate. For example, the RhoA and RhoA kinase (ROCK) signaling pathway in mesenchymal stem cells [18] has been shown to control cell roundness or spreading, where RhoA and ROCK activity is higher in spread cells than round cells, and activation of this activity results in commitment of mesenchymal stem cells to an osteogenic lineage even when cultured in adipogenic differentiation media. Conversely, turning off RhoA and RhoA kinase activity results in commitment to an adipogenic fate, even when cultured in osteogenic differentiation media. Furthermore, in conjunction with TGFβ3, control of the differentiation of MSCs to chondrogenic or smooth muscle cell (SMC) fates also depends on cell shape [11]. In addition, the phenotype of adipose derived stem cells, including proliferation rate, multipotency, and differentiation potential,

depends on early culture conditions [7]; in contrast, the proliferation rate of the C3T10H1/2 model MSC line cells of our studies is independent of, while early markers of differentiation are dependent on, cell density and/or means of achieving density (culture protocol). Another recent study showed differential effects of BMP-6 containing culture medium on adipose derived mesenchymal stem cells cultured in monolayer *versus* pellet culture conditions, where BMP promotes osteogenesis in monolayer and chondrogenesis in pellet cultures [14], underscoring the importance and interplay of both biochemical and biophysical cues on stem cell shape and fate [14,20], and potentially demonstrating intrinsic differences between intramembranous and endochondral ossification related to "spatial dependence of inductive biochemical cues from the ectoderm (an epithelial sheet) and their interplay with biophysical cues deriving from the mesenchymal condensation and proximity to the ectoderm" [20].

Our current results highlight the role biophysical cues play in the commitment of mesenchymal stem cells and the development of skeletal and connective tissues. The process of fate determination likely starts at early time points corresponding physiologically to mesenchymal condensation, the first step in skeletogenesis, which occurs after just 11.5 days of gestation in the mouse [15]. An ideal experiment would investigate the adaptation of mesenchymal stem cells *in situ* as they adapt their shape and the shape of their nuclei in real time. However, due to the complexity of 3D systems and current limitations of 3D cell scale imaging, we used a highly idealized 2D culture model to examine the behavior of these cells in confined or unconfined environments dictated by cell density. In addition, although the impossibility of controlling for temporal cues independent of population doublings is an inherent limitation of the current study (and all studies of this type), plotting pooled cell and nucleus volume as well as shape data, respectively, as a function of time and/or actual density at the time of measurement shows no significant relationship between cell and nucleus shape or volume and time in culture or actual density (where an R^2 greater than 0.8 would indicate a significant relationship, and all R^2values were less than 0.20, Figs. S1, S2). In summary, despite these inherent and current technological limitations, the current study provides a useful means to study the differences in cell and nucleus morphology that result from these two seeding methods.

In fields such as tissue engineering, recent research continues to demonstrate that the recapitulation of biophysical cues such as surface topography [17] or fluid flow induced shear stress [15-17] experienced *in vivo* or during condensation events may be useful for the targeted differentiation of mesenchymal stem cells and the formation of *de novo* tissue. Considering the data presented here, both seeding density and protocol significantly alter the morphology of mesenchymal stem cells even at

very early stages of cell culture. Thus, these design parameters may play a critical role in the success of tissue engineering strategies seeking to recreate condensation events. However, a better understanding of how these changes in cell volume and nucleus shape relate to the differentiation of MSCs is important for prescribing precise seeding conditions necessary for the development of the desired tissue type. In a companion study (Part B, following), we address the effect of concomitant volume and shape changing stresses on spatiotemporal distribution of the cytoskeletal proteins actin and tubulin [3]. Taken together, these studies bring us one step closer to our ultimate goal of elucidating the dynamics of nucleus and cell shape change as tissue templates grow (cell proliferation) and specialize (cell differentiation). An understanding of the relationship between a cell's mechanical environment and its shape and fate may open new possibilities to control cellular structure and function, not only for engineering but also for scale-up in manufacturing of tissue templates.

Conflict of Interest

No benefits in any form have been or will be received from a commercial party related directly or indirectly to the subject of this manuscript. The intellectual property comprising the custom designed flow chamber (and associated novel gasket geometries not) used in this study has been licensed nonexclusively to Warner Instruments, a subsidiary of Harvard Apparatus.

Acknowledgement: This study was supported through a grant from the National Science Foundation (CMMI #0826435). J. Zimmermann was supported through the CMMI grant as well as by Case Western Reserve University's National Science Foundation Research Experience for Undergraduates (REU) grant (EEC-0552804). This investigation was conducted in a facility constructed with support from Research Facilities Improvement Program Grant Number C06 RR12463–01 from the National Center for Research Resources, National Institutes of Health.

References

1. Anderson, E.J., Falls, T.D., Sorkin, A.M., & Knothe Tate, M.L. (2006) *Biomed Eng Online*. 5, 27.

2. Anderson, E.J., & Knothe Tate, M.L. (2007) *Biomed Eng Online*. 6, 46.

3. Chang, H., & Knothe Tate, M.L. (2011) *MCB: Mol Cell Biomech* 187.

4. Dahl, K. N., E. A. Booth-Gauthier, & Ladoux, B. (2010) *J. Biomech.* 43, 2-8.

5. Dunlop, L. L., & Hall, B.K. (1995) *Int. J. Dev. Biol.* 39. 357-371.

6. Engler, A. J., S. Sen, H. L. Sweeny, & Discher, D.E. (2006) *Cell* 126, 677-689.

7. Estes, B.T., Diekman, B.O., & Guilak, F. (2008) *Biotechnol Bioeng* 99, 986-95.

8. Falls, T.D. Beta-catenin's role in the mechanosensitivity of osteochondroprogenitor cells. M.Sc. (Engineering) thesis. Biomedical Engineering, Case Western Reserve University, 2007. Document number: 18263005.

9. Ferguson, C., T. Miclau, D. Hu, E. Alpern, & Helms, J.A. (1998) *Ann NY Acad Sci.* 857, 33–42.

10. Finan, J.D., & Guilak, F. (2010) *J. Cell. Biochem.* 109, 460-467.

11. Gao, L., R. McBeath, & Chen, C. S. (2010) *Stem Cells* 28, 564-572.

12. Guilak, F., J. R. Tedrow, & Burgkart, R. (2000) *Biochem. Biophys. Res. Commun.* 269, 781-786.

13. Katagiri, T, A. Yamaguchi, T. Ikeda, S. Yoshiki, J. M. Wozney, V. Rosen, E.A. Wang, H. Tanaka, S. Omura, & Suda, T. (1990) *Biochem. Biophys. Res. Commun.* 172, 295-299.

14. Kemmis, C.M., Vahdati, A., Weiss, H.E., & Wagner, D.R. (2010) *Biochem. Biophys. Res. Commun.* 401, 20-5.

15. Knothe Tate, M. L., T. D. Falls, S. H. McBride, R. Atit, & Knothe, U.R. (2008) *Int. J. Biochem. Cell Biol.* 40, 2720-2738.

16. Knothe Tate, M., T. Falls, S. K. Mishra, & Atit, R. In: Sivaloganathan, Siv (Ed.) New Perspectives in Mathematical Biology. Toronto: Fields Institute Communications, American Mathematical Society, pp. 113-134.

17. Lim, J. Y., A. E. Loiselle, J.S. Lee, Y. Zhang, J. D. Salvi, and H. J. Donahue. (2011) *J. Orth. Res.* 29, doi: 10.1002/jor.21441.

18. Maniotis, A.J., C.S. Chen, & Ingber, D.E. (1997) *Proc. Natl. Acad. Sci.* USA. 94: 849-854.

19. McBeath R., D. M. Piron, C. M. Nelson, K. Bhadriraju, & Chen, C.S. (2004) *Dev. Cell* 6: 483-495.

20. McBride, S. H., & Knothe Tate, M.L. (2008) *Tissue Eng.* A 14, 1561-1572.

21. McBride, S.H., T. F. Falls, & Knothe Tate, M.L. (2008) *Tissue Eng.* A 14, 1573-1580.

22. Singh, R., J. N. Artaza, W. E. Taylor, N.F. Gonzalez-Cadavid, & Bhasin, S. (2003) *Endocrinology* 144, 5081-5088.

23. Song, M.J., Dean, D., & Knothe Tate, M.L. (2010) *PLoS ONE* 5, e12796.

24. Taylor, S. M., & Jones, P.A. (1979) *Cell* 17, 771-779.

25. Wang, H., G. M. Riha, S. Yan, M. Li, H. Chai, H. Yang, Q. Yao, & Chen, C. (2005) *Atertio. Thromb. Vasc. Biol.* 25, 1817-1823.